Hierarchical Reconstruction with up to Second Degree Remainder for Solving Nonlinear Conservation Laws

Dedicated to Todd F. Dupont on the occasion of his 65th birthday

Yingjie Liu [§], Chi-Wang Shu [¶] and Zhiliang Xu [‡]

Abstract

The hierarchical reconstruction (HR) [Liu, Shu, Tadmor and Zhang, SINUM '07] can effectively reduce spurious oscillations without local characteristic decomposition for numerical capturing of discontinuous solutions. However, there are still small remaining overshoots/undershoots in the vicinity of discontinuities. HR with partial neighboring cells [Xu, Liu and Shu, JCP '09] essentially overcomes this drawback for the third order case, and in the mean time further improves the resolution of the numerical solution. Extending the technique to higher order cases we observe the returning of overshoots/undershoots. In this paper, we introduce a new technique to work with HR on partial neighboring cells, which lowers the order of the remainder of the polynomial in the current cell while maintaining the theoretical order of accuracy, essentially eliminates overshoots/undershoots for the fourth and fifth order cases and reduces the numerical cost.

1 Introduction

Weak solutions of nonlinear conservation laws contain discontinuities, which provide an interesting subject for numerical study and motivate many fundamental numerical techniques, for example, the Godunov scheme [7], MUSCL scheme [25, 26, 27], TVD scheme [8], ENO [9, 23, 24] and WENO schemes [13, 11], and many others. As the formal order of accuracy of a finite volume scheme becomes higher, local characteristic decomposition is usually required. For instance in [17], numerical experiments show that without local characteristic decomposition, spurious oscillations start to show up for both the upwind WENO scheme

[§](E-mail: yingjie@math.gatech.edu)
School of Mathematics, Georgia Institute of Technology, Atlanta, GA 30332. Research supported in part by NSF grant DMS-0810913.

[¶](E-mail: shu@dam.brown.edu)
Division of Applied Mathematics, Brown University, Providence RI 02912. Research supported in part by ARO grant W911NF-08-1-0520 and NSF grant DMS-0809086.

[‡](E-mail: zxu2@nd.edu)
Department of Mathematics, University of Notre Dame, Notre Dame, IN 46556. Research supported in part by NSF grant DMS-0800612.

and a central scheme with WENO reconstruction when the order is higher than three, because the ENO (or WENO) reconstruction locally selects a stencil of cells within the smooth part of the solution to reconstruct a high order polynomial, which is only possible if the solution is decomposed in terms of local characteristic variables in the vicinities of interacting discontinuities. If the numerical solution is represented as a piecewise polynomial, e.g. in the discontinuous Galerkin (DG) method [19, 6, 5, 4], or in a finite volume scheme with a preliminary reconstruction (to generate a piecewise polynomial solution), the WENO strategy can be applied to the cell averages of these polynomials [18]. Compact limiting techniques which are supposed to remove spurious oscillations using information only from adjacent cells for any orders include the TVD/TVB limiter [6], the moment limiter [2] and the recently developed hierarchical reconstruction (HR) [15].

HR decomposes the job of limiting a high order polynomial defined in a cell (which may contain spurious oscillations) into a series of smaller jobs, each of which only involves the non-oscillatory reconstruction of a linear polynomial, e.g. the MUSCL reconstruction. Therefore it only uses information from adjacent cells and can be formulated on unstructured meshes in multi dimensions. It does not use local characteristic decomposition and thus is less dependent on the underlying equation to be solved. Nevertheless in [15, 16], small overshoots/undershoots after interactions of discontinuities can still be observed. HR first takes certain derivative for the polynomials defined in the current cell and its adjacent cells as in the moment limiter. Then it takes a reconstruction approach, namely, it estimates cell averages of the linear part of the polynomial in the current cell over adjacent cells to certain order of accuracy, and applies a non-oscillatory reconstruction to recompute the linear part. The remainder of the polynomial in the current cell (after removing the linear part) plays a key role in estimating cell averages (of the linear part) over adjacent cells. If we only estimate cell averages over partial neighboring cells [30], namely the fraction of adjacent cells (usually half in size) which are closer to the current cell, the remainder in the current cell can be extended over a shorter distance in HR which essentially eliminates overshoots/undershoots in the non-smooth part of the solution in the third order case. However, when the degree of the remainder gets higher (in higher order cases), we may not be able to estimate cell averages of the remainder over smaller partial neighboring cells since it may tolerate more artifacts in the vicinities of interacting discontinuities. This leads us to think of lowering the degree of the remainder in higher order cases. The consideration is to do so without hurting the provable order of accuracy or introducing numerical instability. We would also like to mention that the spectral volume method [28] seems to be more tolerating for limiting techniques. In [31], HR (without using partial neighboring cells) has been successfully applied to the third order spectral volume method on triangular meshes.

2 A Brief Review of the Hierarchical Reconstruction

Here we review the hierarchical reconstruction procedure introduced in [15]. Suppose that the computational domain $\Omega \in R^d$ is a region associated with a mesh $\{C_I : I = 1, 2, \cdots, N\}$, where C_I is called a cell which is a bounded open set with piecewise smooth boundary, $\mathbf{x}_I$ is the centroid of C_I and $\bigcup_{I=1}^{N} \overline{C}_I = \overline{\Omega}$. Let Δx be the maximum of the diameters of C_I for all I. Suppose the numerical solution is represented in each cell C_I by a polynomial $U_I(\mathbf{x} - \mathbf{x}_I)$

of degree r, though it may contain spurious oscillations. The hierarchical reconstruction procedure is to recompute the polynomial $U_I(\mathbf{x}-\mathbf{x}_I)$ by using polynomials in cells adjacent to C_I. These adjacent cells are collected as the set $\{C_J\}$ (which also contains cell C_I) and the polynomials (of degree r) supported on them are thus renamed as $\{U_J(\mathbf{x}-\mathbf{x}_J)\}$ respectively. We need to recompute the new coefficients

$$\frac{1}{\mathbf{m}!}\widetilde{U}_I^{(\mathbf{m})}(\mathbf{0}), \qquad |\mathbf{m}| = r, r-1, \ldots, 0$$

for $U_I(\mathbf{x}-\mathbf{x}_I)$ (written in terms of its Taylor expansion around $\mathbf{x}_I$) iteratively from the highest to the lowest degree terms.

To obtain $\widetilde{U}_I^{(\mathbf{m})}(\mathbf{0})$, we first compute many *candidates* of $U_I^{(\mathbf{m})}(\mathbf{0})$ (sometimes still denoted as $\widetilde{U}_I^{(\mathbf{m})}(\mathbf{0})$ with specification), and we then let the new value for $U_I^{(\mathbf{m})}(\mathbf{0})$ be

$$\widetilde{U}_I^{(\mathbf{m})}(\mathbf{0}) = F\big(\text{ candidates of } U_I^{(\mathbf{m})}(\mathbf{0})\ \big),$$

where F is a convex limiter of its arguments (e.g., the minmod function to be specified later), $F(a_1, a_2, \cdots, a_l) = \sum_{i=1}^{l} \theta_i a_i$, for some $\theta_i \geq 0$ and $\sum_{i=1}^{l} \theta_i = 1$.

In order to find these candidates of $U_I^{(\mathbf{m})}(\mathbf{0})$, $|\mathbf{m}| = m$, we take a $(m-1)^{th}$ order partial derivative of $U_I(\mathbf{x}-\mathbf{x}_I)$ (and also polynomials in adjacent cells), and express

$$\partial^{m-1} U_I(\mathbf{x}-\mathbf{x}_I) = L_I(\mathbf{x}-\mathbf{x}_I) + R_I(\mathbf{x}-\mathbf{x}_I),$$

where L_I is the linear part (containing the zeroth and first degree terms)and R_I is the remainder. Clearly, every coefficient in the first degree terms of L_I is in the set $\{U_I^{(\mathbf{m})}(\mathbf{0}) : |\mathbf{m}| = m\}$. And for every $\mathbf{m}$ subject to $|\mathbf{m}| = m$, one can always take some $(m-1)^{th}$ order partial derivatives of $U_I(\mathbf{x}-\mathbf{x}_I)$ so that $U_I^{(\mathbf{m})}(\mathbf{0})$ is a coefficient in a first degree term of L_I. Thus, a 'candidate' for a coefficient in a first degree term of L_I is the candidate for the corresponding $U_I^{(\mathbf{m})}(\mathbf{0})$.

In order to find a set of candidates for all coefficients in the first degree terms of $L_I(\mathbf{x}-\mathbf{x}_I)$, we only need to know the new approximate cell averages of $L_I(\mathbf{x}-\mathbf{x}_I)$ on $d+1$ distinct mesh cells adjacent to cell C_I. Assume $C_{J_0}, C_{J_1}, \cdots, C_{J_d} \in \{C_J\}$ are these cells and $\overline{L}_{J_0}, \overline{L}_{J_1}, \cdots, \overline{L}_{J_d}$ are the corresponding new approximate cell averages. The set of these $d+1$ cells with the associated cell averages is called a *stencil*. Let a linear polynomial $\widetilde{L}_I(\mathbf{x}-\mathbf{x}_I)$ be determined by the linear system

$$\frac{1}{|C_{J_l}|}\int_{C_{J_l}} \widetilde{L}_I(\mathbf{x}-\mathbf{x}_I)d\mathbf{x} = \overline{L}_{J_l}, \quad l = 0, 1, \cdots, d. \tag{2.1}$$

Then the coefficients in the first degree terms of $\widetilde{L}_I(\mathbf{x}-\mathbf{x}_I)$ become the candidates for the corresponding coefficients of $L_I(\mathbf{x}-\mathbf{x}_I)$. Therefore, a stencil located near cell C_I will determine a set of candidates for all coefficients in the first degree terms of $L_I(\mathbf{x}-\mathbf{x}_I)$. The key is to compute the new approximate cell averages of $L_I(\mathbf{x}-\mathbf{x}_I)$ on the cells of $\{C_J\}$, which is outlined by the following algorithm.

Algorithm 1 Step 1. *Suppose $r \geq 2$. For $m = r, r-1, \cdots, 1$, do the following:*

(a) Take a $(m-1)^{th}$ order partial derivative for each of $\{U_J(\mathbf{x}-\mathbf{x}_J)\}$ to obtain polynomials $\{\partial^{m-1}U_J(\mathbf{x}-\mathbf{x}_J)\}$ respectively. In particular, denote $\partial^{m-1}U_I(\mathbf{x}-\mathbf{x}_I) = L_I(\mathbf{x}-\mathbf{x}_I)+R_I(\mathbf{x}-\mathbf{x}_I)$, where $L_I(\mathbf{x}-\mathbf{x}_I)$ is the linear part of $\partial^{m-1}U_I(\mathbf{x}-\mathbf{x}_I)$ and $R_I(\mathbf{x}-\mathbf{x}_I)$ is the remainder.

(b) For all J, calculate the cell average of $\partial^{m-1}U_J(\mathbf{x}-\mathbf{x}_J)$ on cell C_J to obtain $\overline{\partial^{m-1}U_J}$.

(c) Let $\widetilde{R}_I(\mathbf{x}-\mathbf{x}_I)$ be the $R_I(\mathbf{x}-\mathbf{x}_I)$ with its coefficients replaced by the corresponding new values[1]. For all J, calculate the cell averages of $\widetilde{R}_I(\mathbf{x}-\mathbf{x}_I)$ on the cell C_J to obtain $\overline{R}_J$.

(d) Let $\overline{L}_J = \overline{\partial^{m-1}U_J} - \overline{R}_J$ for all J.

(e) Form stencils out of the new approximate cell averages $\{\overline{L}_J\}$ by using a MUSCL, second order ENO or other non-oscillatory strategies. Each stencil will determine a set of candidates for the coefficients in the first degree terms of $L_I(\mathbf{x}-\mathbf{x}_I)$, which are also candidates for the corresponding $U_I^{(\mathbf{m})}(\mathbf{0})$'s, $|\mathbf{m}| = m$.

(f) Repeat from (a) to (e) until all possible combinations of the $(m-1)^{th}$ order partial derivatives are taken. Then the candidates for all coefficients in the m^{th} degree terms of $U_I(\mathbf{x}-\mathbf{x}_I)$ have been computed. For each of these coefficients, say $\frac{1}{\mathbf{m}!}U_I^{(\mathbf{m})}(\mathbf{0})$, $|\mathbf{m}| = m$, let the new value $\widetilde{U}_I^{(\mathbf{m})}(\mathbf{0}) = F\big(\text{ candidates of } U_I^{(\mathbf{m})}(\mathbf{0})\ \big)$.

Step 2. *The new coefficient in the 0^{th} degree term of $U_I(\mathbf{x}-\mathbf{x}_I)$ is chosen so that the cell average of $U_I(\mathbf{x}-\mathbf{x}_I)$ on cell C_I is invariant with the new coefficients. At this stage all the new coefficients of $U_I(\mathbf{x}-\mathbf{x}_I)$ have been found.*

Even though the non-oscillatory reconstruction of linear polynomials used in Algorithm 1 is only second order accurate (such as the MUSCL or second order ENO), the approximation order of accuracy of a polynomial in a cell is unaffected by the algorithm, because in Step 1(d) the new approximate cell averages satisfy

$$\overline{L}_J = \frac{1}{|C_J|}\int_{C_J} L_I(\mathbf{x}-\mathbf{x}_I)d\mathbf{x} + \mathcal{O}((\Delta x)^{r-m+2}) \tag{2.2}$$

if $\{U_J(\mathbf{x}-\mathbf{x}_J)\}$ have optimal order of approximation to the solution which is locally smooth enough.

3 A Technique to Lower the Degree of the Remainder

Note that in Step 1(c) of Alg. 1, the updated remainder $\widetilde{R}_I(\mathbf{x}-\mathbf{x}_I)$ needs to be averaged outside the cell C_I, which is not a problem in smooth regions of the solution. However, when the involved polynomials contain spurious oscillations, it could cause small overshoots/undershoots from our numerical experience. In the third order case (i.e., $r = 2$ and $\widetilde{R}_I(\mathbf{x}-\mathbf{x}_I)$ can be up to second degree), this problem has been solved in [30] by applying HR with partial neighboring cells (about half of the original size) of C_I so that they are closer to C_I. In higher order cases, $\widetilde{R}_I(\mathbf{x}-\mathbf{x}_I)$ can be above second degree and further bringing

[1] At this stage, we have already found new values for all coefficients in the terms of $U_I(\mathbf{x}-\mathbf{x}_I)$ of degree above m. These coefficients remain in $R_I(\mathbf{x}-\mathbf{x}_I)$ (after taking a $(m-1)^{th}$ order partial of $U_I(\mathbf{x}-\mathbf{x}_I)$). When they are replaced by their corresponding new values, $R_I(\mathbf{x}-\mathbf{x}_I)$ becomes $\widetilde{R}_I(\mathbf{x}-\mathbf{x}_I)$.

partial neighboring cells close to C_I could introduce artifacts near interacting discontinuities of the solution. Simply truncating $\widetilde{R}_I(\mathbf{x}-\mathbf{x}_I)$ to up to second degree will hurt the accuracy. Our new technique uses only second degree terms of $\widetilde{R}_I(\mathbf{x}-\mathbf{x}_I)$ in the estimation of $\overline{L}_J$ when $J \neq I$, and should work with partial neighboring cells for $r \geq 3$.

Algorithm 2 Step 1. *Suppose $r \geq 3$. For $m = r, r-1, \cdots, 1$, do the following:*

(a) Take a $(m-1)^{th}$ order partial derivative for each of $\{U_J(\mathbf{x}-\mathbf{x}_J)\}$ to obtain polynomials $\{\partial^{m-1}U_J(\mathbf{x}-\mathbf{x}_J)\}$ respectively. In particular, denote $\partial^{m-1}U_I(\mathbf{x}-\mathbf{x}_I) = L_I(\mathbf{x}-\mathbf{x}_I)+R_I(\mathbf{x}-\mathbf{x}_I) = L_I(\mathbf{x}-\mathbf{x}_I)+Q_I(\mathbf{x}-\mathbf{x}_I)+\cdots$, where $L_I(\mathbf{x}-\mathbf{x}_I)$ is the linear part of $\partial^{m-1}U_I(\mathbf{x}-\mathbf{x}_I)$, $R_I(\mathbf{x}-\mathbf{x}_I)$ is the remainder and $Q_I(\mathbf{x}-\mathbf{x}_I)$ is the second degree part of the remainder.

(b) Let $\overline{\partial^{m-1}U_I}$ be the cell average of $\partial^{m-1}U_I$ over the cell C_I. For all $J \neq I$, rewrite $\partial^{m-1}U_J(\mathbf{x}-\mathbf{x}_J) = V_J(\mathbf{x}-\mathbf{x}_I) = L_J(\mathbf{x}-\mathbf{x}_I)+Q_J(\mathbf{x}-\mathbf{x}_I)+\cdots$, where $L_J(\mathbf{x}-\mathbf{x}_I)$ is the linear part of $V_J(\mathbf{x}-\mathbf{x}_I)$ and $Q_J(\mathbf{x}-\mathbf{x}_I)$ is the second degree part; calculate the cell average of $L_J(\mathbf{x}-\mathbf{x}_I)+Q_J(\mathbf{x}-\mathbf{x}_I)$ on cell C_J to obtain $\overline{\partial^{m-1}U_J}$.

(c) Let $\overline{R}_I$ be the cell average of $\widetilde{R}_I(\mathbf{x}-\mathbf{x}_I)$ over cell C_I, where $\widetilde{R}_I(\mathbf{x}-\mathbf{x}_I)$ is the $R_I(\mathbf{x}-\mathbf{x}_I)$ with its coefficients replaced by the corresponding new values, similarly for $\widetilde{Q}_I(\mathbf{x}-\mathbf{x}_I)$. For all $J \neq I$, calculate the cell averages of $\widetilde{Q}_I(\mathbf{x}-\mathbf{x}_I)$ on cell C_J to obtain $\overline{R}_J$.

(d) Same as in Alg. 1.

(e) Same as in Alg. 1.

(f) Same as in Alg. 1.

Step 2. *Same as in Alg. 1.*

Remark. In Alg. 2, when $m = r$ and $r-1$, the new coefficients are computed in exactly the same way as in Alg. 1 modulo the differences in Step 1(a), (b) and (c).

Condition 1 *Let $\{\mathbf{x}_{J_0}, \mathbf{x}_{J_1}, \cdots, \mathbf{x}_{J_d}\}$ be the $d+1$ cell centroids of a stencil. Then there is a point among them, say $\mathbf{x}_{J_0}$, such that the matrix $A = \frac{1}{\Delta x}[\mathbf{x}_{J_1}-\mathbf{x}_{J_0}, \mathbf{x}_{J_2}-\mathbf{x}_{J_0}, \cdots, \mathbf{x}_{J_d}-\mathbf{x}_{J_0}]$ is non singular. Further, there is a constant $\beta > 0$ independent of Δx such that $||A^{-1}|| \leq \beta$.*

In 2D, this condition means that $\mathbf{x}_{J_0}, \mathbf{x}_{J_1}, \mathbf{x}_{J_2}$ are not along a straight line. Further, the angles of the triangle $\mathbf{x}_{J_0}, \mathbf{x}_{J_1}, \mathbf{x}_{J_2}$ have a positive lower bound independent of Δx.

Theorem 1 *Suppose $\{U_J(\mathbf{x}-\mathbf{x}_J)\}$ in Algorithm 2 approximate a C^{r+1} function $u(\mathbf{x})$ with point-wise error $\mathcal{O}\big((\Delta x)^{r+1}\big)$ within their respective cell $\{C_J\}$, and all cells in $\{C_J\}$ are contained in a circle centered at $\mathbf{x}_I$ with radius $\mathcal{O}(\Delta x)$. Let the $d+1$ cell centroids in every stencil used in Algorithm 2 satisfy Condition 1. Then after the application of Algorithm 1, the polynomial $\widetilde{U}_I(\mathbf{x}-\mathbf{x}_I)$, i.e. $U_I(\mathbf{x}-\mathbf{x}_I)$ with its coefficients replaced by the corresponding new values also approximates the function $u(\mathbf{x})$ with point-wise error $\mathcal{O}\big((\Delta x)^{r+1}\big)$ within cell C_I. The cell average of $\widetilde{U}_I(\mathbf{x}-\mathbf{x}_I)$ on cell C_I is the same as that of $U_I(\mathbf{x}-\mathbf{x}_I)$.*

Proof. The proof follows [15] exactly once we show that the estimate (2.2) also holds for Algorithm 2. From the assumption we know that the coefficients in the m^{th} degree terms of $U_I(\mathbf{x}-\mathbf{x}_I)$, $0 \leq m \leq r$, are the $(r-m+1)^{th}$ order approximation to the corresponding coefficients of the Taylor expansion of $u(\mathbf{x})$ at $\mathbf{x}_I$.

Assume that when starting to compute new values for the coefficients of the m^{th} degree terms of $U_I(\mathbf{x}-\mathbf{x}_I)$, $1 \le m \le r$, all the computed new values (if there are any) for the coefficients of the l^{th} degree terms ($m < l \le r$, if they exist) of $U_I(\mathbf{x}-\mathbf{x}_I)$ are their $(r-l+1)^{th}$ order approximations respectively. In fact, when $m = r$, there is no new coefficient which has been computed in Step 1 (a). However, the following argument will show that the new values computed in Step 1 (f) for coefficients of the r^{th} degree terms of $U_I(\mathbf{x}-\mathbf{x}_I)$ are their first order approximations respectively.

Let $L_I(\mathbf{x}-\mathbf{x}_I) = c_0 + \mathbf{c}_1 \cdot (\mathbf{x}-\mathbf{x}_I)$ in Step 1 (a) and let $\widehat{L}(\mathbf{x}-\mathbf{x}_I) = \widehat{c}_0 + \widehat{\mathbf{c}}_1 \cdot (\mathbf{x}-\mathbf{x}_I)$ be the corresponding linear part in the Taylor expansion of the same (as for U_J) $(m-1)^{th}$ partial derivative of $u(\mathbf{x})$ at $\mathbf{x}_I$. Therefore c_0 and $\mathbf{c}_1$ approximate $\widehat{c}_0$ and $\widehat{\mathbf{c}}_1$ to the order of $\mathcal{O}\big((\Delta x)^{r-m+2}\big)$ and $\mathcal{O}\big((\Delta x)^{r-m+1}\big)$ respectively. Also from the above assumptions it is easy to see that

$$\begin{array}{l} \overline{R}_I = (1/|C_I|)\int_{C_I} R_I(\mathbf{x}-\mathbf{x}_I)d\mathbf{x} + \mathcal{O}\big((\Delta x)^{r-m+2}\big), \\ \overline{R}_J = (1/|C_J|)\int_{C_J} Q_I(\mathbf{x}-\mathbf{x}_I)d\mathbf{x} + \mathcal{O}\big((\Delta x)^{r-m+2}\big) \ \text{ for } J \ne I, \\ \overline{\partial^{m-1}U_I} = (1/|C_I|)\int_{C_I}[L_I(\mathbf{x}-\mathbf{x}_I) + R_I(\mathbf{x}-\mathbf{x}_I)]d\mathbf{x} \ \text{ and} \\ \overline{\partial^{m-1}U_J} = (1/|C_J|)\int_{C_J}[L_I(\mathbf{x}-\mathbf{x}_I) + Q_I(\mathbf{x}-\mathbf{x}_I)]d\mathbf{x} + \mathcal{O}\big((\Delta x)^{r-m+2}\big) \ \text{ for } J \ne I. \end{array} \tag{3.1}$$

Therefore $\overline{L}_J = \overline{\partial^{m-1}U_J} - \overline{R}_J$ in Step 1 (d) approximates the cell average of $\widehat{L}(\mathbf{x})$ on cell C_J to the order of $O(\Delta x^{r-m+2})$, for all J.

Reconstructing $\widetilde{L}_I(\mathbf{x}-\mathbf{x}_I) = \widetilde{c}_0 + \widetilde{\mathbf{c}}_1 \cdot (\mathbf{x}-\mathbf{x}_I)$ from a stencil $C_{J_0}, C_{J_1}, \cdots, C_{J_d} \in \{C_J\}$ is to find $\widetilde{c}_0$ and $\widetilde{\mathbf{c}}_1$ satisfying the following linear system (see (2.1)),

$$\begin{aligned} \frac{1}{|C_{J_l}|}\int_{C_{J_l}} (\widetilde{c}_0 + \widetilde{\mathbf{c}}_1 \cdot (\mathbf{x}-\mathbf{x}_I))d\mathbf{x} &= \widetilde{c}_0 + \widetilde{\mathbf{c}}_1 \cdot (\mathbf{x}_{J_l} - \mathbf{x}_I) \\ &= \overline{L}_{J_l} = \widehat{c}_0 + \widehat{\mathbf{c}}_1 \cdot (\mathbf{x}_{J_l} - \mathbf{x}_I) + \mathcal{O}\big((\Delta x)^{r-m+2}\big), \end{aligned} \tag{3.2}$$

where $\mathbf{x}_{J_l}$ is the cell centroid of cell C_{J_l}, $l = 0, \cdots, d$. The solutions are candidates for c_0 and $\mathbf{c}_1$ respectively. Subtracting e.g. the first equation ($l = 0$) from the rest of the equations in (3.2) we can obtain

$$A^T(\widetilde{\mathbf{c}}_1 - \widehat{\mathbf{c}}_1) = \mathcal{O}\big((\Delta x)^{r-m+1}\big),$$

where $A = \frac{1}{\Delta x}[\mathbf{x}_{J_1} - \mathbf{x}_{J_0}, \mathbf{x}_{J_2} - \mathbf{x}_{J_0}, \cdots, \mathbf{x}_{J_d} - \mathbf{x}_{J_0}]$. From Condition 1, $||A^{-1}||$ is bounded independent of Δx. We conclude that the candidate

$$\widetilde{\mathbf{c}}_1 = \widehat{\mathbf{c}}_1 + \mathcal{O}\big((\Delta x)^{r-m+1}\big). \tag{3.3}$$

Since the function F used in Step 1 (f) is a convex combination of its arguments, it does not change the approximation order of its arguments. Estimate (3.3) does not involve any new coefficient when $m = r$, thus this shows that the new values computed in Step 1 (f) for the coefficients of the r^{th} degree terms of $U_I(\mathbf{x}-\mathbf{x}_I)$ are their first order approximations respectively. Therefore by induction for $m = r-1, \cdots, 1$, estimate (3.3) implies that the new values for coefficients of the m^{th} degree terms of $U_I(\mathbf{x}-\mathbf{x}_I)$ are their $(r-m+1)^{th}$ order approximations. Along with Step 2, we conclude that $\widetilde{U}_I(\mathbf{x}-\mathbf{x}_I) = u(\mathbf{x}) + \mathcal{O}\big((\Delta x)^{r+1}\big)$ for $\mathbf{x} \in C_I$, and the cell average of $U_I(\mathbf{x}-\mathbf{x}_I)$ on cell C_I is unchanged with the new coefficients. The proof is now complete.

4 Application to 1D Conservation Laws

We now use the finite volume scheme with HR to solve the 1D conservation law

$$\begin{aligned} &\frac{\partial u}{\partial t} + \frac{\partial f(u)}{\partial x} = 0, \quad (x,t) \in R \times (0,T), \\ &u(x,0) = u_0(x), \qquad\qquad x \in R. \end{aligned} \tag{4.1}$$

Let $\{x_i\}$ be a uniform partition in R with $\Delta x = x_{i+1} - x_i$ and $x_{i+1/2} = \frac{1}{2}(x_i + x_{i+1})$. The interval $(x_{i-1/2}, x_{i+1/2})$ is considered as a cell for all i. Integrating (4.1) over $(x_{i-1/2}, x_{i+1/2})$ we obtain

$$\frac{d}{dt}\overline{u_i} = -\frac{1}{\Delta x}\{f(u)|_{x_{i+1/2}} - f(u)|_{x_{i-1/2}}\},$$

where $\overline{u_i}$ is the cell average of u over $(x_{i-1/2}, x_{i+1/2})$. Let $\overline{U_i}$ be the numerical cell average approximating $\overline{u_i}$. Let $\widetilde{U}_i(x)$ be a polynomial defined on $(x_{i-1/2}, x_{i+1/2})$ for all i, reconstructed out of $\{\overline{U_i}\}$. This reconstruction procedure is a major step for a high order finite volume scheme

$$\frac{d}{dt}\overline{U_i} = -\frac{1}{\Delta x}\{F_{i+1/2} - F_{i-1/2}\},$$

where $F_{i+1/2} = h(\widetilde{U}_i(x_{i+1/2}-), \widetilde{U}_{i+1}(x_{i+1/2}+))$ is a flux function. Here we use the Lax-Friedrich flux function $h(a,b) = \frac{1}{2}[f(a)+f(b)] + \frac{\alpha}{2}(a-b)$, where $\alpha = \max_u |f'(u)|$ is the largest characteristic speed, see [22] for more details. We use the third order TVD Runge-Kutta method [23] for the time discretization. For systems of conservation laws, the reconstruction is applied to conservative variables (component-wise) without using local characteristic decomposition.

4.1 Preliminary Reconstruction

Given the numerical cell averages $\{\overline{U_i}\}$ at a time t, we use a central reconstruction to form a piecewise polynomial function $U_i(x)$, $x \in (x_{i-1/2}, x_{i+1/2})$ for all i, although the reconstructed function may contain spurious oscillations in non smooth regions of the solution (see e.g. [16]).

Fourth Order Case. The reconstructed function is a piecewise third degree polynomial ($r = 3$). For convenience, rewrite the reconstructed third degree polynomial in $(x_{i-1/2}, x_{i+1/2})$ as $U_i(x - x_i) = c_0 + c_1(x - x_i) + c_2(x - x_i)^2 + c_3(x - x_i)^3$. The coefficients of this polynomial can be determined by a least-square fit [3, 10]

$$\text{Minimize} \sum_{\{j:0<|j-i|\le 2\}} \Big\{\frac{1}{\Delta x}\int_{x_{j-1/2}}^{x_{j+1/2}} U_i(x - x_i)dx - \overline{U_j}\Big\}^2,$$

$$\text{subject to } \frac{1}{\Delta x}\int_{x_{i-1/2}}^{x_{i+1/2}} U_i(x - x_i)dx = \overline{U_i}.$$

Fifth Order Case. The reconstructed function is a piecewise fourth degree polynomial ($r = 4$). For convenience, rewrite the reconstructed fourth degree polynomial in

$(x_{i-1/2}, x_{i+1/2})$ as $U_i(x - x_i)$. The coefficients of this polynomial can be determined by Solving the following linear system [1]

$$\frac{1}{\Delta x}\int_{x_{j-1/2}}^{x_{j+1/2}} U_i(x - x_i)dx = \overline{U_j},$$

for all j such that $|j - i| \leq 2$.

4.2 Hierarchical Reconstruction

By using a preliminary reconstruction we have obtained a polynomial solution of degree r, $U_i(x - x_i)$, $x \in (x_{i-1/2}, x_{i+1/2})$, for all i. We then apply HR (Alg. 2), to recompute each polynomial and remove possible spurious oscillations. This procedure can also be applied wherever necessary to reduce the cost (see, e.g. [16, 30]), which is out of our focus here. Suppose we want to recompute $U_i(x - x_i)$ in $(x_{i-1/2}, x_{i+1/2})$ to obtain $\widetilde{U}_i(x - x_i)$. Using the partial neighboring cell idea [30] and notations of Alg. 2, we set

$$C_I = (x_{i-1/2}, x_{i+1/2}),$$

$$\{C_J\} = \{(x_{i-1}, x_{i-1/2}), C_I, (x_{i+1/2}, x_{i+1})\},$$

where $(x_{i-1}, x_{i-1/2})$ and $(x_{i+1/2}, x_{i+1})$ are partial neighboring cells where the supported polynomials are still $U_{i-1}(x - x_{i-1})$ and $U_{i+1}(x - x_{i+1})$ respectively. The only two stencils used in Step 1(e) of Alg. 2 are $\{(x_{i-1}, x_{i-1/2}), C_I\}$ and $\{C_I, (x_{i+1/2}, x_{i+1})\}$. The limiter function F of Alg. 2 is taken to be the center biased minmod function [26]

$$F(a, b) = \begin{cases} \min\{(1+\epsilon)a, (1+\epsilon)b, (a+b)/2\}, & \text{if } a, b > 0 \\ \max\{(1+\epsilon)a, (1+\epsilon)b, (a+b)/2\}, & \text{if } a, b < 0 \\ 0, & \text{otherwise} \end{cases}$$

where ϵ is a small perturbation parameter taken to be 0.01 [16] in this paper (see [21, 20] for a discussion for the loss of accuracy due to abrupt shift of stencils, which is the reason for using a perturbation ϵ here).

5 Application to 2D Conservation Laws

The 4^{th} order finite volume implementation on a 2D rectangular grid is similar to the 1D case discussed in the previous section, see [16] for more details. The difference from [16] is that Alg. 2 on partial neighboring cells (instead of Alg. 1) is used. The preliminary reconstruction of a 3^{rd} degree polynomial of two variables on a cell C (left of Fig. 1) is based on a least-square fit over 13 nearby cell averages. In order to eliminate possible spurious oscillations introduced by the preliminary reconstruction, applying HR (Alg. 2) to a cell C_0 (right of Fig. 1) involves 4 partial neighboring cells C_1, C_2, C_3 and C_4 with half of the original size. The polynomial defined on a partial neighboring cell is the same as the one defined on the original cell containing this partial neighboring cell. The stencils used in Alg. 2 are $\{C_0, C_1, C_2\}$, $\{C_0, C_2, C_3\}$, $\{C_0, C_3, C_4\}$ and $\{C_0, C_4, C_1\}$.

Δx	1/10	1/20	1/40	1/80	1/160	1/320	1/640
L_1 *error*	1.10E-4	2.65E-6	1.01E-7	5.31E-9	3.06E-10	1.90E-11	1.18E-12
order	-	5.38	4.71	4.25	4.12	4.01	4.01
L_∞ *error*	1.96E-4	7.48E-6	2.27E-7	1.65E-8	9.99E-10	5.69E-11	3.34E-12
order	-	4.71	5.04	3.78	4.05	4.13	4.09

Table 1: Convergence test for the Burgers equation. 4th order case. Alg. 2 with partial neighboring cells.

Δx	1/10	1/20	1/40	1/80	1/160	1/320
L_1 *error*	2.49E-5	1.60E-7	7.14e-9	2.92E-10	1.02E-11	3.37E-13
order	-	7.28	4.49	4.61	4.84	4.92
L_∞ *error*	7.23E-5	8.65E-7	1.40e-08	5.95E-10	2.71E-11	1.41E-12
order	-	6.39	5.95	4.56	4.46	4.26

Table 2: Convergence test for the Burgers equation. 5th order case. Alg. 2 with partial neighboring cells.

Δx	1/10	1/20	1/40	1/80	1/160	1/320
L_1 *error*	1.99E-5	1.47E-7	6.95E-9	2.87E-10	9.94E-12	3.25E-13
order	-	7.08	4.40	4.60	4.85	4.93
L_∞ *error*	6.00E-5	8.66E-7	1.29E-8	5.59E-10	1.97E-11	6.59E-13
order	-	6.11	6.07	4.53	4.83	4.90

Table 3: Convergence test for the Burgers equation. 5th order case. Alg. 2 with partial neighboring cells in which mixed limiter functions are used.

Δx	1/10	1/20	1/40	1/80	1/160	1/320
L_1 *error*	1.16E-5	9.61E-8	6.47E-9	2.74E-10	9.66E-12	3.22E-13
order	-	6.92	3.89	4.56	4.83	4.91
L_∞ *error*	2.43E-5	1.57E-7	1.27E-8	5.55E-10	1.96E-11	6.56E-13
order	-	7.27	3.63	4.52	4.82	4.90

Table 4: Convergence test for the Burgers equation. 5th order case. Alg. 2 with partial neighboring cells in which the limiter function is replaced by the average of its arguments.

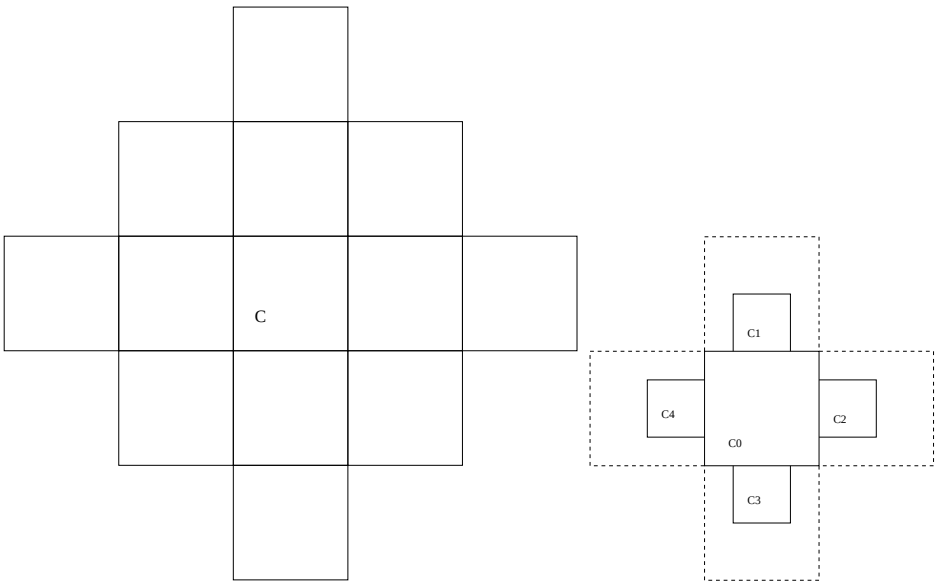

Figure 1: Left: the preliminary reconstruction on cell C depends on 13 nearby cell averages. Right: HR (Alg. 2) for cell C_0 uses 4 partial neighboring cells C_1, C_2, C_3 and C_4.

Δx	1/8	1/16	1/32	1/64	1/128
L_1 *error*	3.03E-3	1.65E-4	7.89E-6	3.87E-7	2.22E-8
order	-	4.20	4.39	4.35	4.12
L_∞ *error*	3.22E-3	2.47E-4	1.08E-5	6.05E-7	4.03E-8
order	-	3.70	4.52	4.16	3.91

Table 5: Convergence test for the 2D Burgers equation. 4th order case. Alg. 2 with partial neighboring cells.

5.1 Numerical Examples

Example 1. We test Alg. 2 with partial neighboring cells by using the Burgers equation $u_t + (\frac{1}{2}u^2)_x = 0$, $u(x,0) = \frac{1}{4} + \frac{1}{2}\sin(\pi x)$. The errors are shown in Tables 1 and 2 at the time $T = 0.1$ when the solution is still smooth. In order to match the spatial order of accuracy, the time step size for the 4^{th} order case is chosen with CFL number 0.9 or as $\Delta x^{4/3}$, whichever is smaller; the time step size for the 5^{th} order case is chosen with CFL number 0.9 or as $\Delta x^{5/3}$, whichever is smaller. Besides the current time step sizes, we have also tried smaller time step sizes and found no significant difference in the error. The convergence rates roughly match the expected orders of convergence at least in the l_1 norm. The order of the l_∞ error for the 5^{th} order case (in Table 2) is gradually reducing to 4 as we refine the mesh. This can be overcome by replacing the limiter function $F(a,b)$ used for recomputing the 4^{th} and 3^{rd} degree coefficients in Alg. 2 by a smoother one described as follows which uses a WENO-type weighted average as in [16]. $F(a,b) = \theta_a a + \theta_b b$, if $ab > 0$; $F(a,b) = 0$ otherwise. Here $\theta_a = [1/(1+\Delta x a^4)]/s$, $\theta_b = [1/(1+\Delta x b^4)]/s$, and $s = [1/(1+\Delta x a^4)] + [1/(1+\Delta x b^4)]$. This

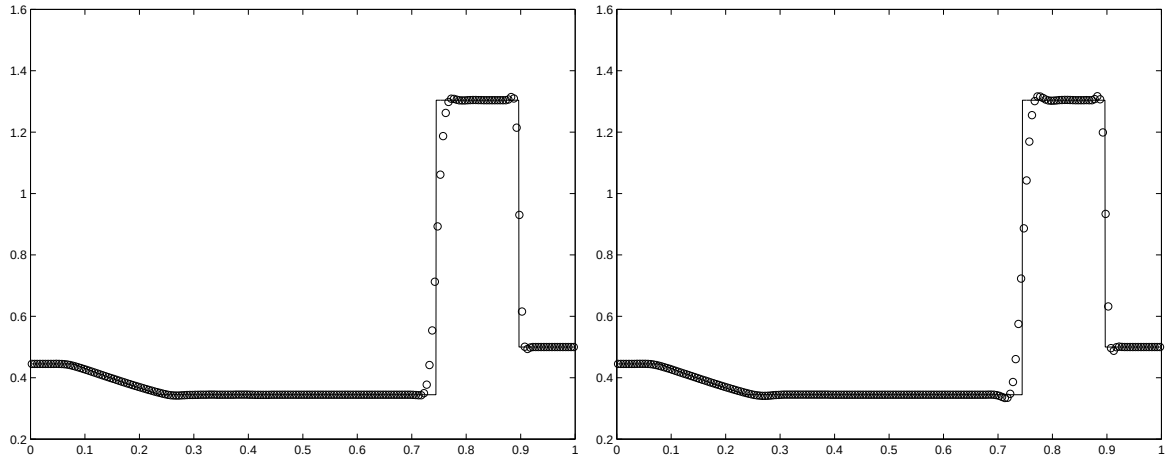

Figure 2: Lax Problem. $N = 200$. 4th order case. Left: Alg. 2 with partial neighboring cells. Right: Alg. 1 without using partial neighboring cells.

ensures that if $a \in \big(\mathcal{O}(\Delta x^{-1}), \mathcal{O}(\Delta x^{-4})\big)$, $b = \mathcal{O}(1)$ and $ab > 0$, then $\theta_a a = \mathcal{O}(\Delta x^2)$ which is within the approximation error order of the 4^{th} and 3^{rd} degree coefficients. We call them the mixed limiter functions and use them to obtain better l_∞ error in Table 3. In fact, the errors in Table 3 are very close to those of Table 4 in which the limiter functions are all set to be $F(a,b) = \frac{1}{2}(a+b)$ without any limiting.

Example 2. Consider the two-dimensional Burgers equation with periodic boundary conditions:

$$\begin{array}{ll} \partial_t u + \partial_x(\frac{u^2}{2}) + \partial_y(\frac{u^2}{2}) = 0, & \text{in } (0,T)\times\Omega\ , \\ u(t=0,x,y) = \frac{1}{4} + \frac{1}{2}\sin(\pi(x+y)), & (x,y)\in\Omega\ , \end{array} \tag{5.1}$$

where $\Omega = [-1,1]\times[-1,1]$. At $T = 0.1$ the exact solution is smooth. We test the 4^{th} order finite volume scheme with Alg. 2 and partial neighboring cells (Sec. 5) on rectangular grids. The time step is taken with CFL number 0.5 or as $\Delta x^{4/3}$, whichever is smaller. The errors at the time $T = 0.1$ are listed in Table 5, which clearly show the 4^{th} order convergence rate.

Example 3. We compute the Euler equations with Lax's initial data [12]. $u_t + f(u)_x = 0$ with $u = (\rho, \rho v, E)^T$, $f(u) = (\rho v, \rho v^2 + p, v(E+p))^T$, $p = (\gamma-1)(E - \frac{1}{2}\rho v^2)$ and $\gamma = 1.4$. Initially, the density ρ, momentum ρv and total energy E are 0.445, 0.311 and 8.928 in $(0, 0.5)$; and are 0.5, 0 and 1.4275 in $(0.5, 1)$. With the CFL number equal to 0.9 and $\Delta x = 1/200$, the computed results are shown at the time $T = 0.16$ in Fig. 2, 3 and the left of Fig. 6. The solid line reference solution is the analytic solution to the Riemann problem. We observe that overshoots/undershoots are essentially eliminated with Alg. 2 on partial neighboring cells. Also the two different limiter functions used in the 5^{th} order case make almost no difference in the graphs.

Example 4. Shu-Osher problem [24]. It is the Euler equations with an initial data

$$\begin{array}{rcl} (\rho, v, p) & = & (3.857143,\ 2.629369,\ 10.333333), \quad \text{for } x < -4, \\ (\rho, v, p) & = & (1 + 0.2\sin(5x),\ 0,\ 1), \quad \text{for } x \geq -4. \end{array}$$

The density profiles are plotted at the time $T = 1.8$ in Fig. 4, 5 and the right of Fig. 6, with $\Delta x = 1/40$ and the CFL number equal to 0.9. The solid line is the numerical solution

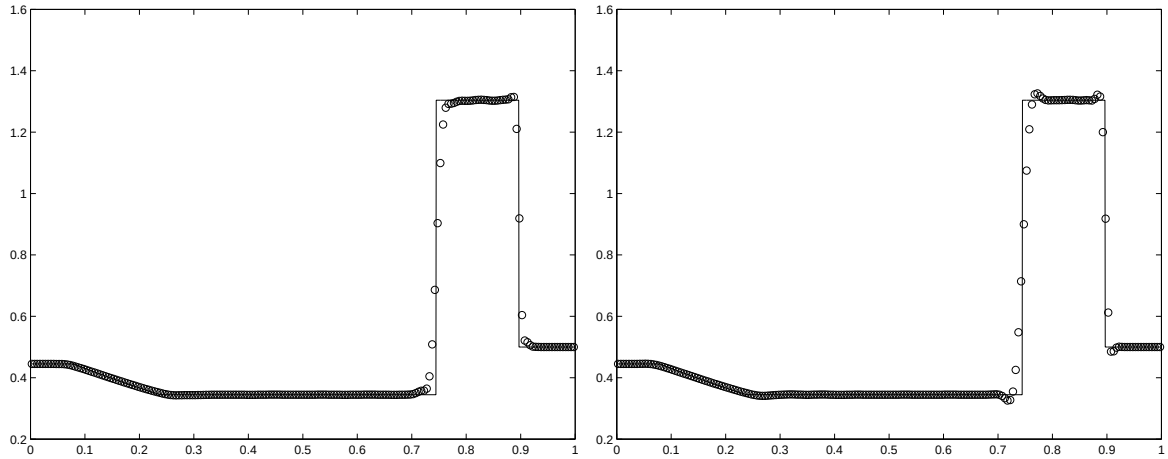

Figure 3: Lax Problem. $N = 200$. 5th order case. Left: Alg. 2 with partial neighboring cells. Right: Alg. 1 without using partial neighboring cells.

on a fine mesh ($\Delta x = 1/200$) computed by a central scheme on overlapping cells [14]. We observe better resolution with Alg. 2 on partial neighboring cells. Also the two different limiter functions used in the 5^{th} order case make almost no difference in the graphs.

Example 5. We compute the 2D Euler equations with the initial data of Lax (example 3), or Shu and Osher (example 4) set along the x-direction, constant initial data along any y-direction, and 0 y-velocity. The 2D Euler equations can be written as

$$\mathbf{u}_t + \mathbf{f}(\mathbf{u})_x + \mathbf{g}(\mathbf{u})_y = 0,\ \mathbf{u} = (\rho, \rho u, \rho v, E)^T,\ p = (\gamma - 1)(E - \tfrac{1}{2}\rho(u^2 + v^2))$$
$$\mathbf{f}(\mathbf{u}) = (\rho u, \rho u^2 + p, \rho uv, u(E + p))^T,\ \mathbf{g}(\mathbf{u}) = (\rho v, \rho uv, \rho v^2 + p, v(E + p))^T,$$

where $\gamma = 1.4$. The density profiles along the x-direction are plotted in Fig. 7, computed by the 4^{th} order finite volume scheme on rectangular grids with Alg. 2 and partial neighboring cells (Sec. 5). The CFL number is equal to 0.5. Clearly, the graphs are similar to their 1D versions in the left of Fig. 2 and the left of Fig. 4.

Example 6. We compute the Double Mach reflection [29] by the 4^{th} order finite volume scheme using Alg. 2 and partial neighboring cells (Sec. 5). It is governed by the 2D Euler equations with the following initial data. A planar Mach 10 shock is incident on an oblique wedge at a $\pi/3$ angle. The air in front of the shock has density 1.4, pressure 1 and velocity 0. The boundarys condition are described in [29].

The CFL number is equal to 0.5. The density profile is plotted at $T = 0.2$ in the top of Fig. 8 with 30 equally spaced contours. The comparative result with Alg. 1 [16] is plotted in the bottom of Fig. 8. It is clear that the top graph shows more rolling in the Mach stem. A fix of negative pressure is necessary for this test problem in [16] with Alg. 1, which is due to the high pressure ratio across strong shocks and overshoots/undershoots. However, using Alg. 2 on partial neighboring cells here, we never detect any negative pressure, which is clearly attributed to the reduction of overshoots/undershoots. In all simulations of this example, HR is only applied in the non smooth region as in [16] in order to reduce the computational cost.

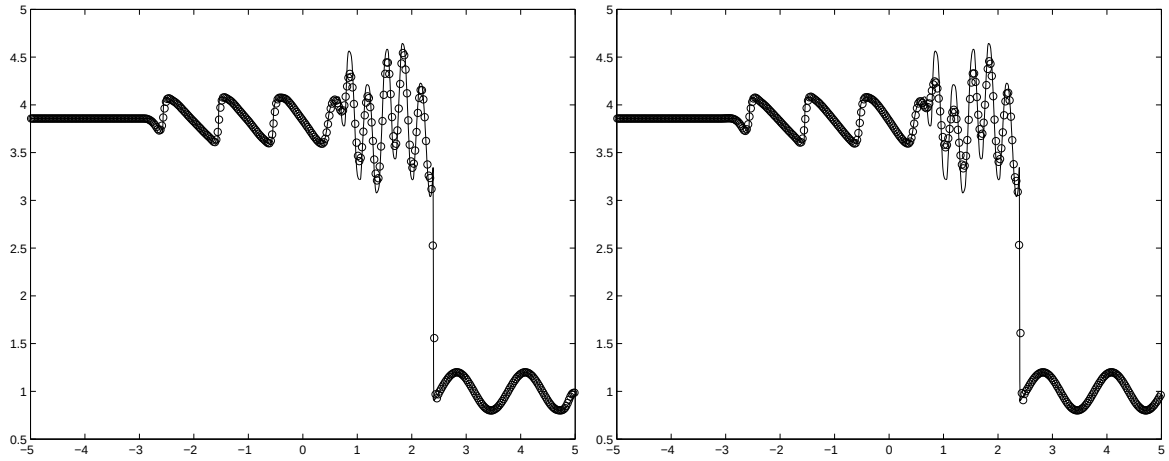

Figure 4: Shu-Osher Problem. $N = 400$. 4th order case. Left: Alg. 2 with partial neighboring cells. Right: Alg. 1 without using partial neighboring cells.

References

[1] R. Abgrall, On essentially non-oscillatory schemes on unstructured meshes: analysis and implementation, *J. Comput. Phys.*, 114 (1994), 45–58.

[2] R. Biswas, K. Devine and J. Flaherty, Parallel, adaptive finite element methods for conservation laws, *Appl. Numer. Math.*, 14 (1994), 255–283.

[3] T. Barth and P. Frederickson, High order solution of the Euler equations on unstructured grids using quadratic reconstruction, *AIAA Paper*, No. 90-0013, (1990).

[4] B. Cockburn and C.-W. Shu, The TVB Runge-Kutta local projection discontinuous Galerkin finite element method for conservation laws V: multidimensional systems, *J. Comput. Phys.*, 141 (1998), 199–224.

[5] B. Cockburn, S.-Y. Lin and C.-W. Shu, TVB Runge-Kutta local projection discontinuous Galerkin finite element method for conservation laws III: one dimensional systems, *J. Comput. Phys.*, 84 (1989), 90–113.

[6] B. Cockburn and C.-W. Shu, TVB Runge-Kutta local projection discontinuous Galerkin finite element method for conservation laws II: general framework, *Math. Comp.*, 52 (1989), 411–435.

[7] S. K. Godunov, *Mat. Sb.*, 47 (1959), 357.

[8] A. Harten, High resolution scheme for hyperbolic conservation laws, *J. Comput. Phys.*, 49 (1983), 357–393.

[9] A. Harten, B. Engquist, S. Osher and S. Chakravarthy, Uniformly high order accurate essentially non-oscillatory schemes, III, *J. Comput. Phys.*, 71 (1987), 231–303.

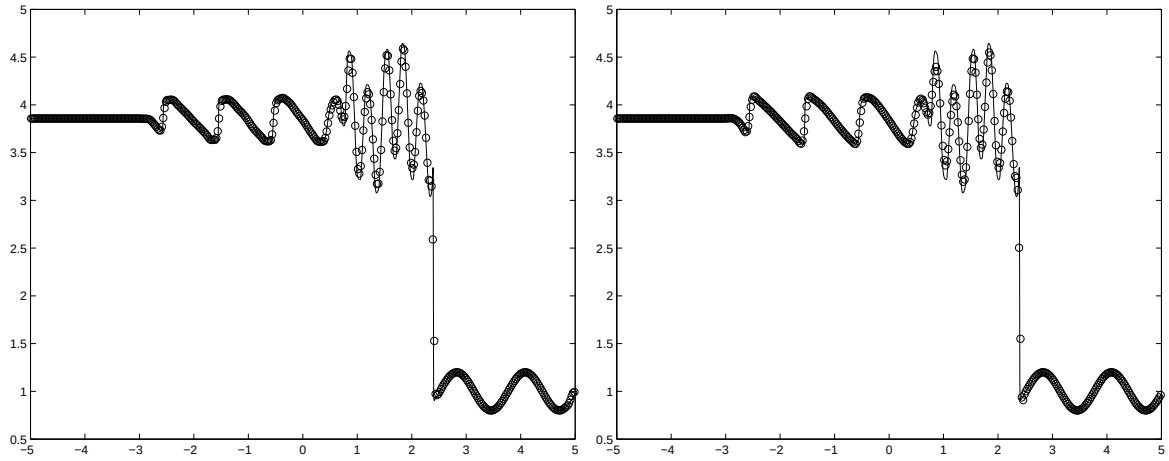

Figure 5: Shu-Osher Problem. $N = 400$. 5th order case. Left: Alg. 2 with partial neighboring cells. Right: Alg. 1 without using partial neighboring cells.

[10] C.-Q. Hu and C.-W. Shu, Weighted essentially non-oscillatory schemes on triangular meshes, *J. Comput. Phys.*, 150 (1999), 97–127.

[11] G.-S. Jiang and C.-W. Shu, Efficient implementation of weighted ENO schemes, *J. Comput. Phys.*, 126 (1996), 202–228.

[12] P. Lax, Weak solutions of nonlinear hyperbolic equations and their numerical computations, *Comm. Pure Appl. Math.*, 7 (1954), 159.

[13] X.-D. Liu, S. Osher and T. Chan, Weighted essentially non-oscillatory schemes, *J. Comput. Phys.*, 115 (1994), 200–212.

[14] Y.-J. Liu, Central schemes on overlapping cells, *J. Comput. Phys.*, 209 (2005), 82–104.

[15] Y.-J. Liu, C.-W. Shu, E. Tadmor and M.-P. Zhang, Central discontinuous Galerkin methods on overlapping cells with a non-oscillatory hierarchical reconstruction, *SIAM J. Numer. Anal.*, 45 (2007), 2442–2467.

[16] Y.-J. Liu, C.-W. Shu, E. Tadmor and M.-P. Zhang, Non-oscillatory hierarchical reconstruction for central and finite volume schemes, *Comm. Comput. Phys.*, 2 (2007), 933–963.

[17] J. Qiu and C.-W. Shu, On the construction, comparison, and local characteristic decomposition for high-order central WENO schemes, *J. Comput. Phys.*, 183 (2002), 187–209.

[18] J. Qiu and C.-W. Shu, Runge-Kutta discontinuous Galerkin method using WENO limiters, *SIAM J. Sci. Comput.*, 26 (2005), 907–929.

[19] W. Reed and T. Hill, Triangular mesh methods for the neutron transport equation, *Tech. report la-ur-73-479*, Los Alamos Scientific Laboratory, 1973.

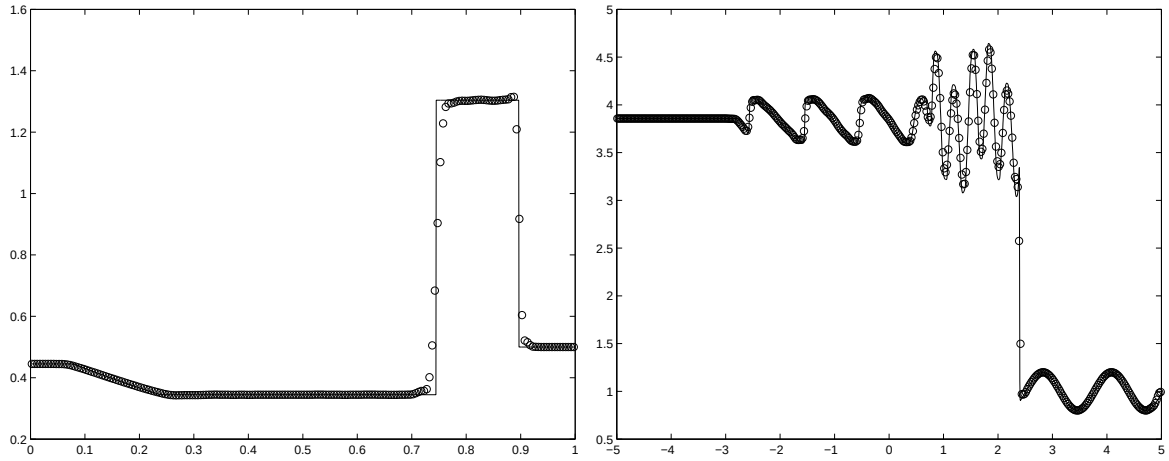

Figure 6: Alg. 2 with partial neighboring cells. 5th order case with mixed limiter functions. Left: Lax problem, $N = 200$. Right: Shu-Osher Problem. $N = 400$.

[20] A.M. Rogerson and E. Meiburg, A numerical study of the convergence properties of ENO schemes, *J. Sci. Comput.*, 5 (1990), 151–167.

[21] C.-W. Shu, Numerical experiments on the accuracy of ENO and modified ENO schemes, *J. Sci. Comput.*, 5 (1990), 127–149.

[22] C.-W. Shu, Essentially non-oscillatory and weighted essentially non-oscillatory schemes for hyperbolic conservation laws, *In Advanced Numerical Approximation of Nonlinear Hyperbolic Equations, B. Cockburn, C. Johnson, C.-W. Shu and E. Tadmor (Editor: A. Quarteroni), Lecture Notes in Mathematics, Berlin. Springer.* , (1998), 1697.

[23] C.-W. Shu and S. Osher, Efficient implementation of essentially non-oscillatory shock capturing schemes, *J. Comput. Phys.*, 77 (1988), 439–471.

[24] C.-W. Shu and S. Osher, Efficient implementation of essentially non-oscillatory shock capturing schemes, II, *J. Comput. Phys.*, 83 (1989), 32–78.

[25] B. van Leer, Toward the ultimate conservative difference scheme: II. Monotonicity and conservation combined in a second order scheme, *J. Comput. Phys.*, 14 (1974), 361–370.

[26] B. van Leer, Towards the ultimate conservative difference scheme: IV. A new approach to numerical convection, *J. Comput. Phys.*, 23 (1977), 276–299.

[27] B. van Leer, Towards the ultimate conservative difference scheme: V. A second order sequel to Godunov's method, *J. Comput. Phys.*, 32 (1979), 101–136.

[28] Z.J. Wang and Y. Liu, Spectral (finite) volume method for conservation laws on unstructured grids III: extension to one-dimensional systems, *J. Sci. Comput.*, 20 (2004), 137–157.

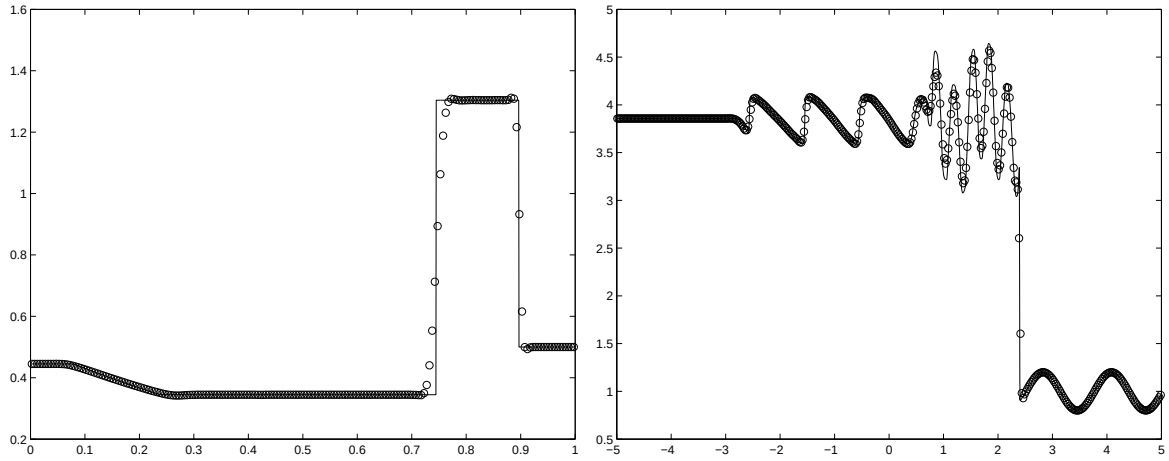

Figure 7: Alg. 2 with partial neighboring cells on 2D rectangular grid. 4th order case. Density profile along the x-direction. Left: Lax problem, $\Delta x = \Delta y = 1/200$. Right: Shu-Osher Problem, $\Delta x = \Delta y = 1/40$.

[29] P. Woodward and P. Colella, Numerical simulation of two-dimensional fluid flows with strong shocks, *J. Comput. Phys.*, 54 (1984), 115.

[30] Z.-L. Xu, Y.-J. Liu and C.-W. Shu, Hierarchical reconstruction for discontinuous Galerkin methods on unstructured grids with a WENO type linear reconstruction and partial neighboring cells, *J. Comput. Phys.*, 228 (2009), 2194–2212.

[31] Z.-L. Xu, Y.-J. Liu and C.-W. Shu, Hierarchical reconstruction for spectral volume method on unstructured grids, *J. Comput. Phys.*, 228 (2009), 5787–5802.

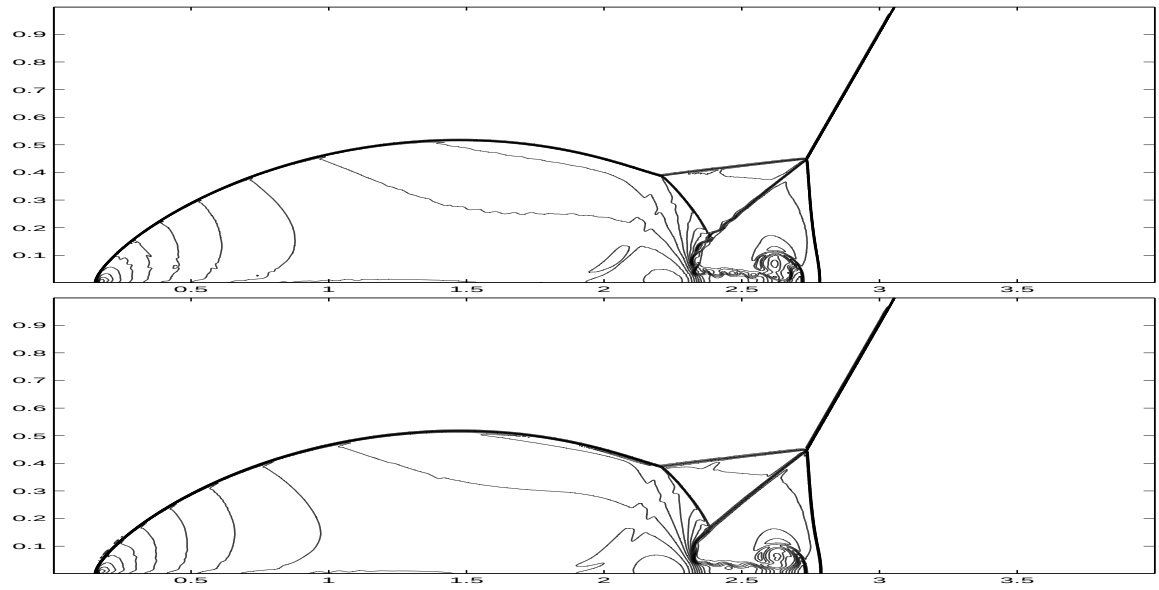

Figure 8: Density contour of Double Mach reflection, 4th order case, $\Delta x = \Delta y = 1/480$. Top: Alg. 2 with partial neighboring cells. Bottom: Alg. 1.